

# Swelling-Deswelling Microencapsulation-Enabled Ultrastable Perovskite–Polymer Composites for Photonic Applications

Ziqian He,<sup>[a]</sup> Juan He,<sup>[a]</sup> Caicai Zhang,<sup>[b, c]</sup> Shin-Tson Wu,<sup>\*[a]</sup> and Yajie Dong<sup>\*[a, b, c]</sup>

**Abstract:** Metal halide perovskite nanocrystals are emerging as novel optoelectronic materials. Owing to their excellent optical and electronic properties such as tunable band gap, narrow-band emission and high charge mobility, they are quite promising in various fields including liquid-crystal display backlighting, solid-state lighting and other energy conversion applications. However, the intrinsic low formation energy makes them vulnerable to external stimulus, e.g. water, oxygen, heat, etc. Among many methods, swelling-deswelling microencapsulation emerges as one of the most promising strategies to improve their stability. Herein, recent developments and future research directions in swelling-deswelling microencapsulation-enabled ultrastable perovskite–polymer composites are summarized. We believe this strategy has great potential to deliver successful perovskite-based commercial products for many photonics applications.

**Keywords:** perovskite nanocrystals, swelling-deswelling microencapsulation, polymer, ultrastable, photoluminescence

## 1. Introduction

Three-dimensional (3D) metal halide perovskites with formula  $ABX_3$  in which A stands for  $Cs^+$ ,  $CH_3NH_3^+$ , or  $CH(NH_2)_2^+$ , B for  $Pb^{2+}$  or  $Sn^{2+}$ , and X for  $Cl^-$ ,  $Br^-$  or  $I^-$ , particularly those in nanocrystal forms, are emerging as highly efficient, bandgap tunable photonics materials.<sup>[1–6]</sup> These perovskite nanocrystals (PNCs) can be easily solution processed at low cost and a photoluminescence quantum yield (PLQY) larger than 90% has been obtained for PNCs in solution with emission linewidths narrower than 20 nm.<sup>[5,6]</sup> Through halide composition tuning, emission over the entire visible band can be realized. With all these advantageous properties, they are

becoming a rising star for displays, solid-state lighting or other energy conversion applications.<sup>[7–11]</sup> However, the quick degradation of PNCs under external stresses or upon colloidal aggregations has been one of the key issues that impedes their practical applications.<sup>[12–14]</sup>

The instabilities of PNCs are often attributed to their low formation energy ( $\sim 0.1$ – $0.3$  eV) induced by the ionic nature, which enables their easy formation, for example, by solution processes but also makes them vulnerable to surface reactions, ion migration, or phase segregation.<sup>[15]</sup> It has been reported that the perovskite grains grow spontaneously even at room temperature in the presence of moisture and oxygen, forming larger grains and resulting in a higher density of defects and a shorter carrier lifetime.<sup>[16]</sup>

To tackle the instability issue, efforts have been made in engineering the composition of PNCs by choosing different cations or preparing different phases, yet the success is limited.<sup>[17]</sup> Other than engineering of perovskite material itself, several passivation strategies have been developed to stabilize perovskites as well as to enhance the brightness of perovskites, but still cannot fully solve the environmental instability issue. For instance, the introduction of surfactants and ligands into PNC synthesis can achieve passivation of individual nanocrystal grains and result in colloidal perovskites with enhanced

[a] Z. He, J. He, Dr. S.-T. Wu, Dr. Y. Dong  
College of Optics and Photonics, University of Central Florida,  
Orlando, Florida 32816, USA  
E-mail: swu@creol.ucf.edu  
Yajie.Dong@ucf.edu

[b] C. Zhang, Dr. Y. Dong  
Department of Materials Science & Engineering, University of  
Central Florida, Orlando, Florida 32816, USA

[c] C. Zhang, Dr. Y. Dong  
NanoScience Technology Center, University of Central Florida,  
Orlando, Florida 32826, USA

stability and PLQY.<sup>[18]</sup> However, the reaction yield of PNCs remains low and when the PNCs are processed as thin films, their efficiency reduced substantially because of the spontaneous particle aggregation-induced quenching.<sup>[19]</sup> Moreover, postsynthetic treatments are needed to withstand environmental stresses, such as the employment of silica or polymer coatings on PNCs.<sup>[20–25]</sup> A very promising method is to encapsulate PNCs with some water- or/and oxygen-proof matrices. One commonly used approach involves crystallization and growth of PNCs in a preformed mesoporous inorganic matrix by solution process.<sup>[26–28]</sup> However, the preformed inorganic porous structures will inevitably lead to partially exposed, unprotected perovskites. Thus, the protection of PNCs against water and oxygen is very limited. Moreover, comparing to other non-templated matrices, the use of template will complicate the process and increase the cost. By contrast, polymer matrix-protected PNCs become more and more popular due to the plethora of polymer choices and

large variability of polymer properties. Among many polymer matrix-based stabilization or in-situ fabrication strategies of PNCs,<sup>[29–32]</sup> swelling-deswelling encapsulation is a unique and valuable class, because the fabrication process is extremely simple and the choices of suitable polymers are abundant, which in turn ensures the low cost and good environmental stability.

Here, we review the exploration of the polymer swelling-deswelling microencapsulation (SDM) process that enables the dispersion, in-situ crystallization, and subsequent surface passivation of perovskite nanocrystals in polymer matrices. With the help of polymer matrices, ultrastable metal halide perovskite-polymer composites (PPCs) with outstanding optical properties can be generated, which can be suitable for various efficient and highly reliable photonics applications. The future research and development of this strategy will also be discussed.



Ziqian He received his BS degree from the College of Engineering and Applied Sciences at Nanjing University, Nanjing, China, in 2016. He is currently working toward his PhD degree at the College of Optics and Photonics, University of Central Florida, Orlando, FL, USA. His research focuses on perovskite nanomaterials, liquid-crystal devices and displays.



Juan He received her BS and MS degrees from the Department of Physics at Peking University, Beijing, China, in 2011 and 2014, respectively. She is currently working toward her PhD degree at the College of Optics and Photonics, University of Central Florida, Orlando, FL, USA. Her research focuses on quantum dots and perovskite light-emitting materials for display, sensing and lasing applications.



Caicai Zhang received her BS degree in Physical Science and Technology department from Lanzhou University in 2013, her MS degree in Materials Science and Engineering from University of Florida in 2016, and is currently working toward her PhD degree in Materials Science and Engineering at University of Central Florida. Her current research focuses on metal halide perovskite luminescent materials and devices for display, lighting, and other novel applications.



Shin-Tson Wu is a Pegasus professor at College of Optics and Photonics, University of Central Florida. He is among the first six inductees of the Florida Inventors Hall of Fame (2014), and a Charter Fellow of the National Academy of Inventors (2012). He is a Fellow of the IEEE, OSA, SID, and SPIE, and the recipient of 2014 OSA Esther Hoffman Beller medal, 2011 SID Slottow-Owaki prize, 2010 OSA Joseph Fraunhofer award, 2008 SPIE G. G. Stokes award and 2008 SID Jan Rajchman prize.



Yajie Dong is an assistant professor in NanoScience Technology Center of University of Central Florida, with joint appointment in College of Optics and Photonics and Department of Materials Science & Engineering. He received his BS and MS degrees in Chemistry from Tsinghua University, Beijing, China, and his PhD degree from Harvard University. He is an associate editor of Optics Express and a member of the Emissive Display (EMD) subcommittee of the SID Technical Program Committee.

## 2. Development of SDM

### 2.1. Polymer Films Based SDM

It is well known that crosslinked polymers can swell when in contact with or immersed in good solvents and such solvents can penetrate into the polymers with the solutes. The swelling of the polymers is generally reversible through a deswelling process which can be achieved by evaporating the solvent or washing by theta solvent.<sup>[33]</sup> Previously, polymer swelling-deswelling processes have been applied to encapsulate bioactive drugs into polymer matrices as solutes and enable controllable release of the drugs.<sup>[34,35]</sup> In light of this principle, we hypothesize that perovskite precursors can also be introduced into polymer matrices as solute through the polymer swelling process (Figure 1a). The precursors start to crystallize and grow when the solvent is driven out of the polymer matrix, for example, by baking. Meanwhile, the polymer matrix will deswell and shrink, forming a strong barrier layer for the PNCs to protect them from water, oxygen or heat from the surrounding environment.

Our first demonstration of SDM-enabled PPCs was based on organic-inorganic perovskites ( $\text{MAPbBr}_3$ ,  $\text{MA} = \text{CH}_3\text{NH}_3^+$ ) and dimethylformamide (DMF) was applied as the precursor solvent.<sup>[36]</sup> To demonstrate the generality of SDM, several technically important polymer substrates including polystyrene (PS), polycarbonate (PC), acrylonitrile butadiene styrene (ABS), cellulose acetate (CA), polyvinyl chloride (PVC), and poly(methyl methacrylate) (PMMA), were tested (Figure 1b–c). Polymer swelling was achieved through either cotton swab brushing on static polymer substrates (Figure 1b) or dynamic spin-coating where precursor solution was deposited onto the high-speed spinning substrates (Figure 1c). The deswelling process was fulfilled by subsequent annealing of the substrates. Visible color changes from transparent (for most polymers) or semi-clear (for ABS film) to light green can be observed, indicating PNC formations along with solvent evaporation and polymer deswelling.

It is natural to think that for different polymer substrates under the same treatment condition, the end results in terms of PNC grain size distribution, PLQY, loading ratio and environmental stability can be different. Even for the same polymer but with different crosslinking level, the results can vary a lot. In experiments, most of the polymers were readily swelled except PMMA. From the top-view scanning electron microscopy (SEM) images, only PMMA shows PNCs on the surface which can be easily washed away by water. Other polymers encapsulated PNCs successfully and exhibited water-resistance in some extents depending largely on the water permeability of the substrates themselves. The difference is from the swelling ratio of the solvent in different polymers. Later we found that the same PMMA substrates that cannot be swelled well using dynamic spin can be decently swelled by

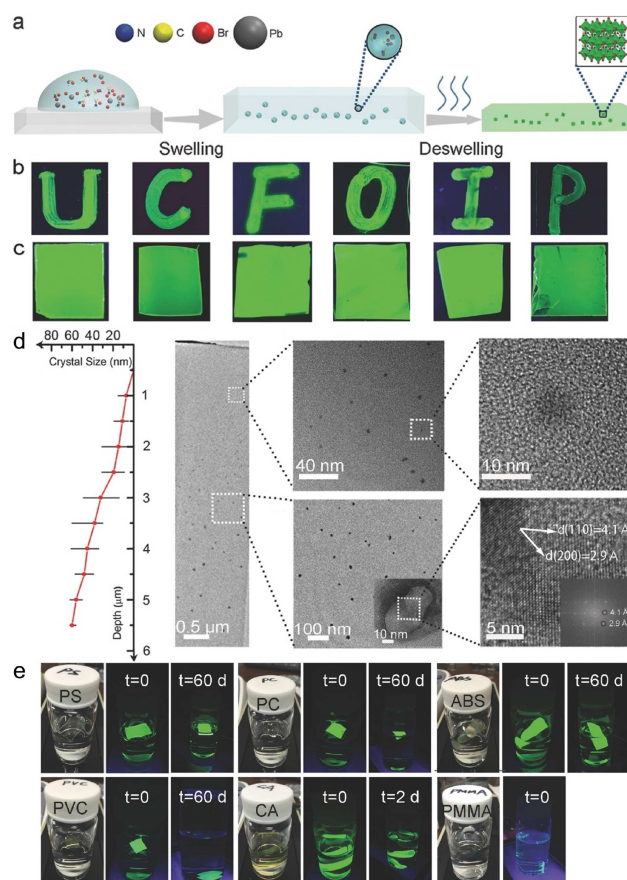


**Figure 1.** Swelling-deswelling microencapsulation strategy to perovskite-polymer composites. a) Scheme of  $\text{MAPbBr}_3$ -polymer composite formation process through swelling-deswelling. b, c) Images of the luminescent composite samples prepared by cotton swab painting (b) or spin coating (c) under UV excitation (365 nm). Samples from left to right are  $\text{MAPbBr}_3$ -PS,  $\text{MAPbBr}_3$ -PC,  $\text{MAPbBr}_3$ -ABS,  $\text{MAPbBr}_3$ -CA,  $\text{MAPbBr}_3$ -PVC and  $\text{MAPbBr}_3$ -PMMA respectively. d) Maximum, minimum and average size distribution of nanocrystal along with depth from the top surface and cross-section TEM images of  $\text{MAPbBr}_3$ -PS showing the depth-dependent size-varied  $\text{MAPbBr}_3$  nanoparticles embedded in PS. e) Photographs taken under white light or UV irradiation at indicated time period. The composite film samples immersed in water are  $\text{MAPbBr}_3$ -PS,  $\text{MAPbBr}_3$ -PC,  $\text{MAPbBr}_3$ -ABS,  $\text{MAPbBr}_3$ -PVC,  $\text{MAPbBr}_3$ -CA, and  $\text{MAPbBr}_3$ -PMMA. Reproduced by permission of John Wiley and Sons, Copyright 2016.<sup>[36]</sup>

immersing the substrates into the precursor solution, and water-resistant PMMA PPCs can be realized by subsequent annealing of the substrates.

Thanks to the relatively rigid polymer substrates, PNCs inside the polymers are well-dispersed and passivated, and thus phase segregations can be avoided. Interestingly, the crystal size varies from several nm to  $>60$  nm as the embedding depth increases from several hundred nm to  $>5$   $\mu\text{m}$ , as observed in the  $\text{MAPbBr}_3$ -PS sample (Figure 1d). This might be interpreted by the speed variations in the deswelling process as a function of embedding depth. It is harder to evaporate the

precursor solution deeper inside the polymer matrix, and thus the precursor droplets are freer to coalesce, and PNCs can grow larger. The broad crystal size distribution can be unwanted in traditional semiconductor quantum dots (QDs), since the emission peak wavelength depends on the size and a broad size distribution will lead to a broad emission spectrum. However fortunately, PNCs are quite insensitive to the quantum confinement. Even with such a broad size distribution, a full width at half maximum (FWHM) of less than 20 nm can be readily achieved. Such narrow emission bandwidths are crucial for display and lighting applications.

Most intriguingly, this simple in-site fabrication strategy of PPCs offers very good environmental stability to the vulnerable PNCs. MAPbBr<sub>3</sub> capsulated in PS, PC, PVC and ABS substrates showed less than 7% PLQY decay after immersed in water for two months (Figure 1e). The heating-cooling test demonstrated that MAPbBr<sub>3</sub>-PS and MAPbBr<sub>3</sub>-PC can fully recover after being heated up to 100 and 110 °C, respectively. Even immersed in boiling water for 30 min, the MAPbBr<sub>3</sub>-PC and MAPbBr<sub>3</sub>-PS samples manifested merely less than 7% and 15% PLQY decay, respectively.

Applying the same strategy, when the precursors change to inorganic CsPbBr<sub>3</sub>, in-situ formation of perovskite nanorods (PNR) can be fulfilled inside the polymer matrices.<sup>[37]</sup> As the CsPbBr<sub>3</sub> perovskite precursor solution is introduced into the polymer matrix through swelling, it distributes as stripe-shape droplets in between the swollen polymer chains. PNCs start to nucleate and grow as the solvent is driven out from the polymer matrices through annealing and thus PNRs are formed. The PNR formation process takes advantages of polymer matrix passivation and protection. In the experiment, the PNRs were only formed several micrometers underneath the top surface of PS substrates, which ensures their decent encapsulation. The well-protected PNRs showed great long-term environmental stability even without further buffer layers. After being immersed in water for 277 days, the PLQY of PNRs-PS increased from 30% to 40%. Upon heating up to 80 °C and then cooling back to room temperature, the PL emission can be fully recovered. The PNRs-PS sample can even survive in boiling water for 30 s without visible PL decay.

The PNRs can vary in sizes, depending highly on the precursor concentration and dynamic spin speed (Figure 2). Specifically, with higher precursor concentration, the precursor solution is more viscous, leading to larger droplets during SDM process and thus larger PNRs will be formed. Meanwhile, a higher spin speed results in a more dispersive distribution of precursor droplets, which ensures a smaller droplet size in the polymer matrix and thus smaller PNRs will be generated. The PNR size distribution also highly relies on the polymer substrate itself. As PS, PC and ABS are all capable of creating PNRs, even with the same precursor concentration and spin speed, the PNR sizes are different. This means the

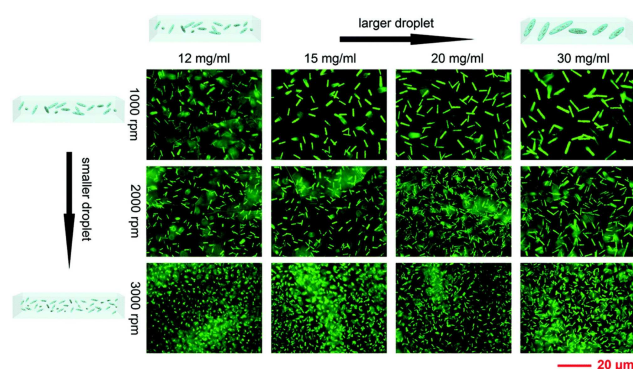


**Figure 2.** Fluorescence microscopy images of PNRs-PS synthesized with different precursor concentrations and different spin-coating speeds. Focal planes were adjusted to be ~4–5 μm underneath the top surface for all samples. The insets on the top and left are schematic illustrations for the droplet size under different conditions. Reproduced by permission of The Royal Society of Chemistry.<sup>[37]</sup>

PNR formation depends on the properties of the polymer itself, including swelling ratio, cross-linking level, cluster morphology, etc.

Although the PNRs with anisotropic shapes show partially polarized emission, their random orientations inside the polymer matrices will cancel out the polarization properties of the emission. As the PNRs formed by the SDM strategy are randomly oriented, macroscopic alignment is crucial to achieve polarized emission. Thanks to the outstanding stability of the PNRs inside the polymer substrates and the plastic deformation ability of the polymers, macroscale alignment can be achieved upon stretching the polymer substrates at an elevated temperature. In the experiment, a CsPbBr<sub>3</sub>-PS film was stretched to 8 times longer the initial length after heated up by a heat gun. After the stretch, 37% of them lie in the ±1.5° range and 80% of them lie in the ±4.5° range with respect to the stretching direction. The PNRs with orientation order will provide partially polarized emission, which is useful for liquid-crystal display (LCD) backlight. In this particular case, the PNRs can result in 24% higher light transmittance comparing to non-polarized emission. However, the major drawback of this alignment method is the decreased mechanical robustness of the polymer substrate.

Inspired by the SDM strategy, a recent work by Shi, et al demonstrated patterned PNCs in polymer substrates by in-situ inkjet printing.<sup>[38]</sup> By dropping the perovskite precursor solution ink onto the polymer substrates and applying subsequent drying, PNC patterns with dot pixels down to 100's μm can be realized (Figure 3a). Comparing with a prior report by Liu, et al that demonstrated PNC patterning by printing solution containing polyvinyl pyrrolidone (PVP) and perovskite precursors,<sup>[39]</sup> the in-situ inkjet printing based on SDM can achieve PNC patterns with higher stability against

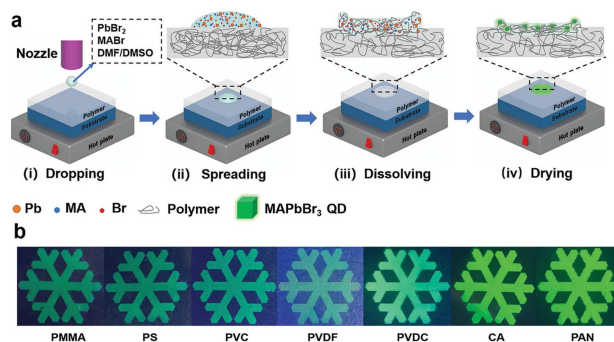


**Figure 3.** a) Schematic diagram of the in-situ inkjet printing strategy. b) The optical images of printed PNC patterns on different polymer substrate under UV light. Reproduced by permission of John Wiley and Sons, Copyright 2019.<sup>[35]</sup>

moisture and can be applied to a variety of polymers. MAPbBr<sub>3</sub> based PNC patterns have been successfully created on PMMA, PS, PVC, polyvinylidene fluoride (PVDF), polyvinylidene chloride (PVDC), CA, and polyacrylonitrile (PAN) substrates with PLQY up to 80% (Figure 3b). The patterned MAPbBr<sub>3</sub>-PVDC can still be luminescent after being immersed into water for 100 days. Other than MA based PNCs, CsPbBr<sub>3</sub> and FAPbBr<sub>3</sub> (FA = HC(NH<sub>2</sub>)<sub>2</sub><sup>+</sup>) PNCs can also be patterned, which again proves the generosity of this method. It was also revealed that the morphology of the pixels is coffee ring and the size of the pixels depends on the temperature of the substrates where the average pixel size decreases from 212 to 100 μm as the substrate temperature increases from 30 to 90 °C. With the ability of generating full-color patterns, the SDM-based inkjet printing can be useful for displays and anti-counterfeiting.

## 2.2. Polymer Beads Based SDM

So far, we have emphasized on applying the SDM strategy to polymer films. Nevertheless, the variety of the polymer form factors will boost the potential of this strategy. In 2017, Lin and coworkers demonstrated the so-called swelling-shrinking strategy to achieve superior water resistance, by encapsulating pre-synthesized PNCs into crosslinked PS polymer beads.<sup>[40]</sup> This strategy is essentially the same as SDM. After the PS beads were swelled by PNC-containing toluene, the solvent was removed by high-speed centrifugation or vacuum evaporating. Then, instead of applying annealing, they utilized theta solvent, hexane, containing an equal concentration of PNCs to realized deswelling and prevent PNC leaking from PS matrices. After another low-speed centrifugation, the final PNC-PS composite beads were fabricated. Although the encapsulation showed almost no influence on the crystal structure, it has profound impact on the optical properties. Notably, the peak

wavelengths of the PNC-PS composites were shifted, and the bandwidths were enlarged compared with the bare PNCs. The PNC-PS composites can prevent anion exchange when mixing composites with different colors, and were still highly luminescent (for green samples) after stored in water for more than nine months.

Although the previous work demonstrated PNC-PS beads with high water resistance, the multi-step synthesis and the waste of materials during swelling and deswelling will inevitably result in rigorous restrictions on polymer choices and relatively high costs. To overcome these issues, our group recently developed a one-step synthesis method of polymer beads based PPCs (Figure 4a).<sup>[41]</sup> By fully mixing perovskite precursors (CsPbBr<sub>3</sub>), ligands (oleylamine and oleic acid) and polymer beads (PS or PMMA), the luminescent PPCs can be quickly and easily generated through injecting an antisolvent (e.g. isopropyl alcohol (IPA), toluene, etc.) into the mixture. After another centrifugation and vacuum drying, the final PPCs were obtained. The synthesis only took a few seconds at room temperature and almost all the perovskite and polymer materials were utilized, thus assuring its low cost. This method also releases the requirements of polymer, as long as the polymer can be partially swelled by the solvent (e.g. DMF) of perovskite precursors.

Through adjusting the perovskite precursor composition, a group of PNC-PS composites were obtained, with their emission spectra covering the entire visible band (Figure 4b). The SEM and transmission electron microscopy (TEM) images showed that the PNCs are essentially anchored on the polymer beads, instead of fully encapsulated inside the beads. This should be ascribed to an insufficient swelling process. However surprisingly, even though the PNCs are not well enveloped, the PNC-PS composites still exhibit superior water resistance. The green PNC-PS only experienced PL decay for the first several days which can be attributed to the decay of

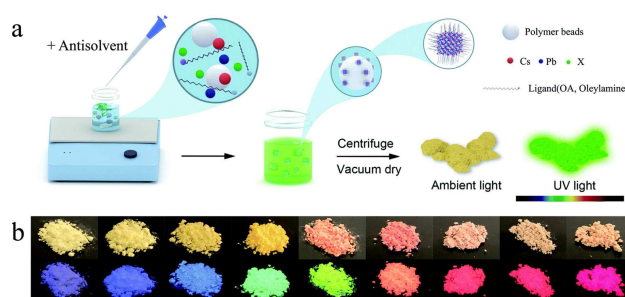


**Figure 4.** Schematic illustration of the fabrication process of light-diffusing, downconverting perovskite-polymer composites (PPCs). (a) After a one-step synthesis of PPCs through antisolvent-induced heterogeneous nucleation, the powders can be obtained by further centrifugation and vacuum drying. (b) Images of PPCs with different anion compositions under ambient light (upper) and 365 nm UV light (lower) illumination. Reproduced by permission of The Royal Society of Chemistry.<sup>[41]</sup>

some freestanding PNCs, and then became stable. After being immersed in water for over 50 days, the relative PL intensity maintained  $\sim 80\%$ . Even for the relatively unstable red samples, the PL intensity remained  $\sim 60\%$  after 50 days. More interestingly, the PNC–PS composite can even survive in boiling water.

The superior water stability can be partially explained by the incomplete SDM process where parts of the PNCs are inside and thus protected by the polymer beads. Another mechanism leading to such water resistance should be the formation of air nanobubbles at the interface between water and the hydrophobic polymer bead surface that prevent PNCs from directly contacting water. It was reported that stable nanobubbles could be formed on a solid surface when immersed into certain liquids and such nanobubbles formed on hydrophobic surfaces should be more stable than those formed on hydrophilic surfaces.<sup>[42–44]</sup> Thanks to the hydrophobic nature of the polymer beads, the PNC–PS composites can be stable in water even if SDM is inadequate. Moreover, the PNC–PS composites exhibited even higher hydrophobicity than the PS beads. Specifically, the contact angle of the PS beads is  $131.7^\circ$ , while that of PNC–PS composites increases to  $146.7^\circ$ . This increase is probably due to the large hydrophobicity of the surfactant oleylamine attached on the PNC–PS composites. This super-hydrophobicity makes the PNC–PS composites even more stable in water. By contrast, the green-emitting PNCs synthesized without hydrophobic polymer beads and with otherwise identical conditions were quickly decayed in water at room temperature. Although the PNC–PS composites already manifested good water stability, it is worth pointing out that to further enhance the environmental stability, it is desirable to have complete SDM where PNCs are fully enveloped in the polymer matrices. To achieve that, one may apply less crosslinked polymers or use other swelling conditions.

### 3. Potential Applications

In the recent decade, PNCs have been intensively explored as the next-generation optoelectronic materials due to their excellent electronic and optical properties. However, the PPCs currently developed by the SDM strategy are more similar to a guest-host system, which may limit their adoption in some applications such as solar cells or electrically driven light-emitting diodes (LEDs). But given that the SDM-based PPCs exhibit superior stability against environmental stimulus, structural stability by passivation of the polymer matrix, and large degree of freedom on matrix choices, utilizing SDM-based PPCs in optoelectronic or electrooptical applications can be a future direction, for example, to boost the operation lifetime of perovskite LEDs which is their bottle neck at this

moment.<sup>[45]</sup> Nevertheless, here in this section, we will focus on the PL-related applications that are currently targeted and discuss in detail about the applications that have huge market shares such as displays and advanced lighting.

#### 3.1. Liquid Crystal Displays and Other Displays

As the display color gamut evaluation metrics keep upgrading from sRGB, via NTSC (National Television Standards committee), and now to Rec. 2020,<sup>[46]</sup> the traditional phosphor-converted white LEDs as LCD backlight can no longer meet the requirement. To fulfill this demand, some narrow-band downconverters such as QDs and potassium fluorosilicate KSF/PFS phosphors have been applied in commercial products. PNCs as a new kind of narrow-band PL materials are highly promising to compete with them. But their vulnerability against environmental stimulus prevented them from practical applications. By the SDM strategy, ultrastable PPCs with very low cost can be achieved. Comparing with the Cd-based QDs (emission bandwidth 20–30 nm),<sup>[47]</sup> the green-emitting PPC can easily obtain  $< 20$  nm emission bandwidth. Moreover, Cd is considered much more toxic than Pb. According to the Restriction of Hazardous Substances (RoHS), the maximum Cd content is limited to 100 ppm in any consumer electronic product while the maximum allowable Pb content is one order of magnitude larger (1000 ppm).<sup>[48]</sup> Therefore, PPCs seem to be a very attractive substitute for pure green colors over QDs and phosphors (bandwidth  $\sim 55$  nm). As for red colors, the currently developed PPCs are still inferior to QDs and KSF/PFS phosphors as the emission bandwidth is about 35–40 nm, the structural and environmental stability is not as good as the green ones and the PL quantum efficiency remains relatively low (“red wall”).<sup>[49]</sup> Another concern is that although SDM can provide superior environmental stability, thermo quenching (PL intensity drops as temperature increases) is still prohibiting on-chip uses of PNCs.

Based on the above analysis, three hybrid configurations of edge-lit LCD backlight have been proposed, as shown in Figure 5. With a spectral optimization considering the LC mode, the polarizer, the analyzer, and the color filters, a maximum Rec. 2020 color gamut coverage of 92.8% can be realized for the first configuration (Figure 5a).<sup>[8]</sup> In fact, similar color performance can be obtained by all three configurations, as the color purity requirement for red colors has more tolerance and the color gamut becomes mainly limited by the color filters when ultra narrow-band emitters are employed.

Beside the mature edge-lit LCDs, PPCs are also promising in the rising direct-lit mini-LED LCDs for high dynamic range displays.<sup>[50]</sup> Similar to the edge-lit counterpart, remote PNC film with remote red QD film or on-chip red phosphor can be utilized. However, these approaches still need to overcome

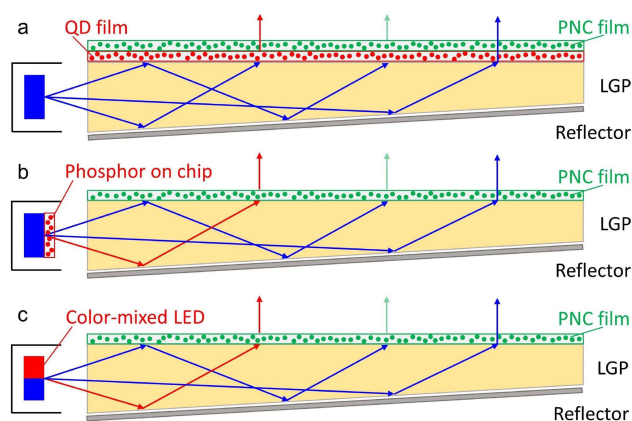


**Figure 5.** Schematic diagram of three different hybrid configurations implementing on-surface PNC films with (a) on-surface red quantum-dots (QD) film; (b) on-chip red phosphor; (c) color-mixed LED chips for edge-lit LCD backlight. LGP: lightguide plate. Reproduced from Ref. [8].

challenges such as yellow rings (for a particular zone, the periphery region becomes yellowish) or slow PL decay time of KSF/PFS phosphors.

It should be noted that for PPC films to be utilized in display applications, homogeneity, film thickness and nanocrystal loading ratio control will be crucial. The homogeneity is controlled by both the swelling and deswelling processes. For small-size films, spin-coating can guarantee good uniformity. However, for large-size films, blade-coating or slot-die coating may be a better choice. On the other hand, the thickness of the composite film is determined by the diffusion depth of perovskite precursors in the polymer substrate during swelling and can be tuned in a certain range to meet the requirement of different display applications. Currently, free-standing composite films with thickness ranging from 30 to several hundred micrometers have been fabricated with high stability and good uniformity. There are indeed some thickness limitations of this method. Since the swelling-deswelling process happens from the surface, it will be difficult to achieve complete nanocrystal microencapsulation and conversion of bulky polymer substrates with thickness in the mm to cm range or above. Fortunately for the film thickness meaningful for display (tens to several hundred micrometers), the approach has proved to be effective. On the other hand, the nanocrystal loading ratio might be limited by the swelling ratio of the polymers. But it can be varied by tuning the perovskite concentration in the precursor solution in a range. For LCD backlight, the loading ratio can meet the requirement to generate a white light.

For more general display applications, it is worth mentioning that although there are possibilities for PPCs to be used in self-emissive displays such as organic LEDs (OLEDs) and micro LEDs as color converters, much effort is needed to

achieve high optical density (e.g. 2), pixelize the down-converters and in the meantime reduce the color crosstalk, and reduce the ambient excitation, etc.

### 3.2. Solid-State Lighting and Beyond

In the early stage of solid-state lighting (SSL), researches have been devoted into pushing the efficiency while maintaining high color rendering quality.<sup>[51]</sup> However, in the current stage, SSL starts to aim at beyond energy saving, such as human circadian lighting or horticultural lighting.<sup>[52]</sup> For those applications, the ability to tailoring the spectral power distribution (SPD) of the light sources in accordance to specific requirements while keeping high efficiency becomes critical. For example, a good human circadian lighting source needs to provide the correct circadian action, by taking the circadian action spectrum into design consideration.<sup>[53]</sup> The narrow-band and color-tunable emitters will offer more spectrum design freedom, where the PPCs can meet such requirements and even lower the cost by the easy process, low material costs and the capability of combining downconverters with diffusers. Based on the optical properties of PPCs, spectral optimizations have been performed for  $RG_pB$  (red, blue LEDs plus green PNC downconverted blue LEDs) and  $RY_pG_pB$  (red, blue LEDs plus yellow, green PNC downconverted blue LEDs) SSL sources that are healthy in circadian rhythm, excellent in color rendering, and highly efficient (Figure 6a–b).<sup>[8,9]</sup> As shown in Figure 6c, both optimized solutions are highly efficient, and can even offer better circadian variations than standard illuminants. Comparing to three-color SSL, four-color SSL can obtain much better color rendering quality and thus fulfill the demand for circadian, efficient, good color-rendering SSL.

Other than displays and SSL, PPCs may also find other PL-related applications such as biological labeling and imaging, lasing, X-ray scintillator, luminescent solar concentrators, security phosphor, emissive projection display, etc. As the PPCs have not been optimized for those applications, future researches can target on them and optimize such guest-host systems accordingly.

## 4. Future Development

The SDM-based PPCs offer excellent environmental stability and fairly large design degree of freedom in polymer, solvent, precursor and process choices. But currently this strategy is still in its infancy. There is still huge potential in future research and development, such as understanding the mechanism, exploiting the guest-host system, optimizing device performance according to specific applications, etc.

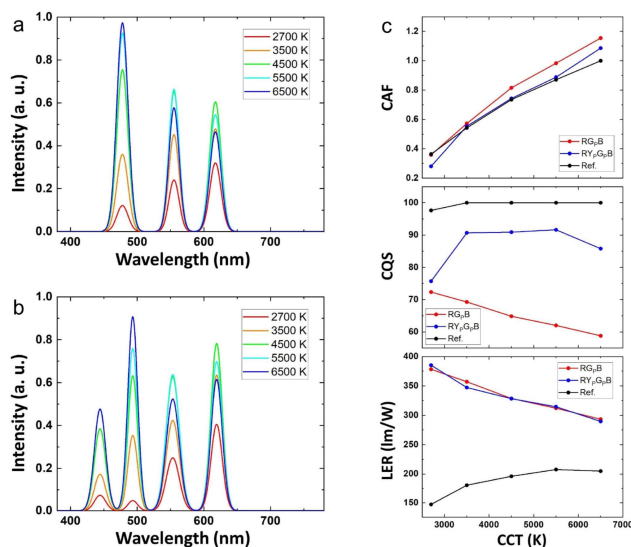


**Figure 6.** SPDs of an optimal solution at different correlated color temperatures (CCTs) for (a) RG<sub>p</sub>B (peak wavelengths: 477.9 nm, 555.1 nm and 617.3 nm) and (b) RY<sub>p</sub>G<sub>p</sub>B (peak wavelengths: 444.2 nm, 493.3 nm, 553.3 nm, and 619.1 nm) type SSL. (c) The detailed performance as a function of CCT. CAF: circadian action factor; CQS: color quality scale; LER: luminous efficacy of radiation; Ref: reference. The reference is a blackbody radiator below 5000 K and a CIE standard illuminant above 5000 K. Reproduced from Ref. [8].

#### 4.1. Understanding the Formation Mechanism

Although the general procedure of SDM can be sketched and understood, it is important to study the PNC formation mechanism. With more knowledge on the solvent dispersion, interaction between precursors and polymer chains/functional groups, and crystal nucleation and growth, better guest-host systems can be established. For example, it is pivotal to investigate in what condition and why anisotropic PNCs will be created such that macroscale alignment of PNCs may potentially be realized without stretching the polymer. It is also important to understand how polymer matrices passivate the PNCs and whether the interaction between polymer chains/functional groups and PNCs determines how stable the PPCs are, since it is intuitive to think polymers that have lower water/oxygen permeability can better prevent water/oxygen induced PNC degradation. To fulfill those tasks, feasible techniques need to be developed and applied to monitor the SDM process as well as the PNC decay process.

#### 4.2. Exploring the Large Variability in SDM

In an SDM process, a lot of variables can play important roles, including the precursor solution, polymer matrices, swelling and deswelling conditions, etc. Specifically, for the precursor solution, the composition and the concentration of the perovskite precursor, whether ligands/surfactants are added or

not, and the choice of solvent will all influence the PNC formation and thus the final optical properties. As for polymer matrices, there are still a lot of other polymer material choices and if we change the precursor solvent, the degree of freedom is even larger. Not only the polymer material itself, but the form factors allow a variety of modifications. For example, the form factors can be rod-shape or even micro structured. There is also space for adjusting the swelling and deswelling process. A prominent example is that the deswelling process can be fulfilled by annealing, theta solvent or others. Optimizing this step can have large impacts on the PNC nucleation and growth, and thus result in different PNC dispersion and optical properties.

#### 4.3. Optimizing the PPCs According to Specific Applications

To meet the requirements for various applications, there is plenty of room for improving the guest-host system. For example, for SSL uses, integrating downconverters with diffusers can even lower the cost and device compactness. Thus, converting the light-diffusing polymer beads into PPCs by SDM will be valuable. As for display uses, upgrading the PNC loading ratio while maintaining the narrow-band emission will be meaningful. But for those applications, stability is still the most important aspect. For the commercially used quantum dot enhancement film (QDEF), extra barrier layers are needed to avoid environment-induced decay. If those barrier layers can be removed for PPCs, they can be even more attractive and competitive. For applications beyond displays and SSL, the requirements can be concentrated on other aspects. As an example, luminescent solar concentrators favor large Stokes shift and low light scattering.<sup>[54]</sup> Therefore, reducing the PNC size and controlling the size dispersion will be crucial.

### 5. Conclusion

The recent advances of SDM-based PPCs is reviewed. Through simple swelling-deswelling process, the PNCs can be well encapsulated into various polymer matrices. Protected and passivated by the polymer chains, the PNCs show much improved stability against environmental stimulus such as water, oxygen, heat, etc., and can even survive in boiling water. This strategy offers large degree of freedom in perovskite precursor, solvent, ligand/surfactant, and polymer choices. The exploration of this strategy is still in its infancy and we believe that it has great potential to deliver perovskite-based commercial products to the display and/or lighting markets in the near future.

## Acknowledgements

The authors thank Dr. Andre J. Gesquiere, Dr. Yongho Sohn, Dr. Lei Zhai for helpful discussions and assistance in materials characterizations. S. T. Wu acknowledges partial support of AFOSR under contract No. FA9550-14-1-0279. Y. Dong is grateful for support of this work by UCF through startup funding (Grant No. 20080738) and a NSTC seed grant (No. 63014223).

## References

- [1] A. Kojima, K. Teshima, Y. Shirai, T. Miyasaka, *J. Am. Chem. Soc.* **2009**, *131*, 6050.
- [2] A. Kojima, M. Ikegami, K. Teshima, T. Miyasaka, *Chem. Lett.* **2012**, *41*, 397.
- [3] L. C. Schmidt, A. Pertegás, S. González-Carrero, O. Malinkiewicz, S. Agouram, G. Mínguez Espallargas, H. J. Bolink, R. E. Galian, J. Pérez-Prieto, *J. Am. Chem. Soc.* **2014**, *136*, 850.
- [4] G. Li, Z. K. Tan, D. Di, M. L. Lai, L. Jiang, J. H. W. Lim, R. H. Friend, N. C. Greenham, *Nano Lett.* **2015**, *15*, 2640.
- [5] L. Protesescu, S. Yakunin, M. I. Bodnarchuk, F. Krieg, R. Caputo, C. H. Hendon, R. X. Yang, A. Walsh, M. V. Kovalenko, *Nano Lett.* **2015**, *15*, 3692.
- [6] F. Zhang, H. Z. Zhong, C. Chen, X. G. Wu, X. M. Hu, H. L. Huang, J. B. Han, B. S. Zou, Y. P. Dong, *ACS Nano* **2015**, *9*, 4533.
- [7] J. He, H. Chen, J. Chen, Y. Wang, S. T. Wu, Y. Dong, *Opt. Express* **2017**, *25*, 12915.
- [8] Z. He, C. Zhang, Y. Dong, S. T. Wu, *Crystals* **2019**, *9*, 59.
- [9] Z. He, C. Zhang, H. Chen, Y. Dong, S. T. Wu, *Nanomaterials* **2019**, *9*, 176.
- [10] Q. Chen, J. Wu, X. Ou, B. Huang, J. Almudraq, A. A. Zhumekenov, X. Guan, S. Han, L. Liang, Z. Yi, J. Li, X. Xie, Y. Wang, Y. Li, D. Fan, D. B. L. Teh, A. H. All, O. F. Mohammed, O. M. Bakr, T. Wu, M. Bettinelli, H. Yang, W. Huang, X. Liu, *Nature* **2018**, *561*, 88.
- [11] M. Wei, F. P. G. de Arquer, G. Walters, Z. Yang, L. N. Quan, Y. Kim, R. Sabatini, R. Quintero-Bermudez, L. Gao, J. Z. Fan, F. Fan, A. Gold-Parker, M. F. Toney, E. H. Sargent, *Nat. Energy* **2019**, *4*, 197–205.
- [12] T. Leijtens, G. E. Eperon, N. K. Noel, S. N. Habisreutinger, A. Petrozza, H. J. Snaith, *Adv. Energy Mater.* **2015**, *5*, 1500963.
- [13] G. Niu, X. Guo, L. Wang, *J. Mater. Chem. A* **2015**, *3*, 8970.
- [14] B. W. Park, S. I. Seok, *Adv. Mater.* **2019**, *31*, 1805337.
- [15] L. Loo, P. Patel, *MRS Bull.* **2015**, *40*, 636.
- [16] R. Sheng, X. Wen, S. Huang, X. Hao, S. Chen, Y. Jiang, X. Deng, M. Green, A. Ho-Baillie, *Nanoscale* **2016**, *8*, 1926.
- [17] Y. Wei, Z. Cheng, J. Lin, *Chem. Soc. Rev.* **2019**, *48*, 310.
- [18] I. Levchuk, A. Osvet, X. Tang, M. Brandl, J. D. Perea, F. Hoegl, G. J. Matt, R. Hock, M. Batentschuk, C. J. Brabec, *Nano Lett.* **2017**, *17*, 2765.
- [19] F. Zhu, L. Men, Y. Guo, Q. Zhu, U. Bhattacharjee, P. M. Goodwin, J. W. Petrich, E. A. Smith, J. Vela, *ACS Nano* **2015**, *9*, 2948.
- [20] S. Huang, Z. Li, L. Kong, N. Zhu, A. Shan, L. Li, *J. Am. Chem. Soc.* **2016**, *138*, 5749.
- [21] H. Huang, B. Chen, Z. Wang, T. F. Hung, A. S. Sussha, H. Zhong, A. L. Rogach, *Chem. Sci.* **2016**, *7*, 5699.
- [22] C. Sun, Y. Zhang, C. Ruan, C. Yin, X. Wang, Y. Wang, W. W. Yu, *Adv. Mater.* **2016**, *28*, 10088.
- [23] S. Hou, Y. Guo, Y. Tang, Q. Quan, *ACS Appl. Mater. Interfaces* **2017**, *9*, 18417.
- [24] S. N. Raja, Y. Bekenstein, M. A. Koc, S. Fischer, D. Zhang, L. Lin, R. O. Ritchie, P. Yang, A. P. Alivisatos, *ACS Appl. Mater. Interfaces* **2016**, *8*, 35523.
- [25] H. Zhang, X. Wang, Q. Liao, Z. Xu, H. Li, L. Zheng, H. Fu, *Adv. Funct. Mater.* **2017**, *27*, 1604382.
- [26] S. N. Habisreutinger, T. Leijtens, G. E. Eperon, S. D. Stranks, R. J. Nicholas, H. J. Snaith, *Nano Lett.* **2014**, *14*, 5561.
- [27] V. Malgras, S. Tominaka, J. W. Ryan, J. Henzie, T. Takei, K. Ohara, Y. Yamauchi, *J. Am. Chem. Soc.* **2016**, *138*, 13874.
- [28] D. N. Dirin, L. Protesescu, D. Trummer, I. V. Kochetygov, S. Yakunin, F. Krumeich, N. P. Stadie, M. V. Kovalenko, *Nano Lett.* **2016**, *16*, 5866.
- [29] Y. Ling, Y. Tian, X. Wang, J. C. Wang, J. M. Knox, F. Perez-Orive, Y. Du, L. Tan, K. Hanson, B. Ma, H. Gao, *Adv. Mater.* **2016**, *28*, 8983–8989.
- [30] Y. Xin, H. Zhao, J. Zhang, *ACS Appl. Mater. Interfaces* **2018**, *10*, 4971–4980.
- [31] C. Carrillo-Carrión, P. del Pino, B. Pelaz, *Appl. Mater. Today* **2019**, *15*, 562–569.
- [32] S. Chang, Z. Bai, H. Zhong, *Adv. Opt. Mater.* **2018**, *6*, 1800380.
- [33] B. Erman, P. Flory, *Macromolecules* **1986**, *19*, 2342.
- [34] M. Li, O. Rouaud, D. Poncet, *Int. J. Pharm.* **2008**, *363*, 26.
- [35] S. Freitas, H. P. Merkle, B. Gander, *J. Controlled Release* **2005**, *102*, 313.
- [36] Y. Wang, J. He, H. Chen, J. Chen, R. Zhu, P. Ma, A. Towers, Y. Lin, A. J. Gesquiere, S. T. Wu, Y. Dong, *Adv. Mater.* **2016**, *28*, 10710.
- [37] J. He, A. Towers, Y. Wang, P. Yuan, J. Zhang, J. Chen, A. J. Gesquiere, S. T. Wu, Y. Dong, *Nanoscale* **2018**, *10*, 15436.
- [38] L. Shi, L. Meng, F. Jiang, Y. Ge, F. Li, X. G. Wu, H. Zhong, *Adv. Funct. Mater.* **2019**, 1903648.
- [39] Y. Liu, F. Li, L. Qiu, K. Yang, Q. Li, X. Zheng, H. Hu, T. Guo, C. Wu, T. W. Kim, *ACS Nano* **2019**, *13*, 2042.
- [40] Y. Wei, X. Deng, Z. Xie, X. Cai, S. Liang, P. Ma, Z. Hou, Z. Cheng, J. Lin, *Adv. Funct. Mater.* **2017**, *27*, 1703535.
- [41] C. Zhang, Z. He, H. Chen, L. Zhou, G. Tan, S. T. Wu, Y. Dong, *J. Mater. Chem. C* **2019**, *7*, 6527.
- [42] Y. Sun, G. Xie, Y. Peng, W. Xia, J. Sha, *Colloids Surf. A* **2016**, *495*, 176.
- [43] X. H. Zhang, N. Maeda, V. S. J. Craig, *Langmuir* **2006**, *22*, 5025.
- [44] G. Pan, B. Yang, *ChemPhysChem* **2012**, *13*, 2205.
- [45] X. Zhao, J. D. A. Ng, R. H. Friend, Z. K. Tan, *ACS Photonics* **2018**, *5*, 3866.

- [46] K. Masaoka, Y. Nishida, M. Sugawara, E. Nakasu, *IEEE Trans. Broadcast.* **2010**, *56*, 452.
- [47] H. Chen, J. He, S. T. Wu, *IEEE J. Sel. Top. Quantum Electron.* **2017**, *23*, 1900611.
- [48] "Restriction of the Use of Certain Hazardous Substances in Electrical and Electronic Equipment," EU Directive 2002/95/EC, 2003.
- [49] L. Protesescu, S. Yakunin, S. Kumar, J. Bär, F. Bertolotti, N. Masciocchi, A. Guagliardi, M. Grotevent, I. Shorubalko, M. I. Bodnarchuk, C. J. Shih, M. V. Kovalenko, *ACS Nano* **2017**, *11*, 3119.
- [50] G. Tan, Y. Huang, M. C. Li, S. L. Lee, S. T. Wu, *Opt. Express* **2018**, *26*, 16572.
- [51] T. Taguchi, *IEEE J. Trans. Electr. Electron. Eng.* **2008**, *3*, 21.
- [52] P. M. Pattison, J. Y. Tsao, G. C. Brainard, B. Bugbee, *Nature* **2018**, *563*, 493.
- [53] D. Gall, *Licht* **2002**, *54*, 1292.
- [54] R. Mazzaro, A. Vomiero, *Adv. Energy Mater.* **2018**, *8*, 1801903.

---

*Manuscript received: September 2, 2019*

*Revised manuscript received: November 6, 2019*

*Version of record online: December 13, 2019*